



## A NOVEL COMPUTER SIMULATION TECHNIQUE FOR MODELING GRAIN GROWTH

Long-Qing Chen

Department of Materials Science and Engineering, Pennsylvania State University, University Park, PA 16802

(Received May 16, 1994)

(Revised August 15, 1994)

### Introduction

Grain growth is a process in which the average grain size of a single-phase polycrystalline material increases as a function of time, driven by the reduction in the total grain-boundary energy. Since most advanced materials are polycrystalline, their physical properties, including mechanical and electrical properties, are influenced and very often controlled by the microstructures developed during grain growth following sintering or solidification. Therefore, it is of technological importance to fundamentally understand grain growth kinetics responsible for the temporal microstructural evolution. Over the last half century, there have been many experimental as well as theoretical investigations of grain growth process. Most of the mean-field and statistical theories were summarized in a review paper by Atkinson [1]. They are Burke and Turnbull's analysis based on the mean surface-curvature as the driving force [2], the mean-field theories of Feltham [3], Hillert [4] and Louat [5], the topological analyses of Smith [6], and Rhines and Craig [7], and the statistical theory of Kurtz and Carpay [8]. These theoretical works have greatly improved our understanding of normal grain growth kinetics. However, grain growth in real materials is a very complex process which requires many assumptions in all analytical or statistical theories. Recently, there has been enormous interest in using computer simulations to understand grain growth kinetics. According to Atkinson's classification [1], these computer simulations can be characterized as statistical [9-11], deterministic [12-17] and probabilistic [18-22]. Among them, the Monte-Carlo simulation technique based on the Q-state Potts model [19-22] has emerged as the most popular one which provides a direct simulation of microstructural evolution without tracking the positions of grain boundaries and has been applied to a wide variety of problems [23]. In the Q-state Potts model, a microstructure is discretized using a lattice, with each lattice site assigned a number between 1 and Q representing the crystallographic orientation of a grain. Grain boundaries are located between lattice sites with different orientation numbers and are associated with a grain boundary energy. The movement of grain boundaries is determined by a Monte-Carlo procedure.

In this paper, I propose a new computer simulation model for investigating grain growth kinetics, born from the recent work on the domain growth kinetics of a quenched system with many non-conserved order parameters [24]. A key new feature of this model for studying grain growth is that the grain boundaries are diffuse, as opposed to previous mean-field and statistical theories and Monte-Carlo simulations which assumed that grain boundaries were sharp. Unlike the Monte-Carlo simulations in which grain boundaries are made up of kinks, grain boundaries in our continuum model are smooth. Below, I shall describe this model in detail, give prescriptions for computer simulation, and then present computer simulation results on a two-dimensional model system.

### The Computer Simulation Technique

In contrast to the Q-state Potts model in which a microstructure is represented by a set of discrete integer numbers, a microstructure in this model is described by a set of continuous field variables,  $\eta_1(r), \eta_2(r), \dots, \eta_p(r)$ . Each field variable represents grains of a given crystallographic orientation. They are continuous variables ranging from -1.0 to 1.0. For example, a value of 1.0 for  $\eta_1(r)$  means that the material at position  $r$  has the crystallographic orientation labeled as 1; a value of -1.0, indicates that the material at position  $r$  is anti-phase or 180°-rotation related to orientation 1. At the grain boundary region between orientation 1 and 2,  $\eta_1(r)$  and  $\eta_2(r)$  will have absolute values intermediate between 0.0 and

1.0. To completely describe an arbitrary microstructure requires an infinite number of field variables. However, as I shall demonstrate later, a large but finite number is sufficient for realistically modeling the grain growth kinetics.

In the diffuse interface theory, the total free energy of an inhomogeneous system containing grain boundaries is given by

$$F = F_o + \int \left[ f(\eta_1(r), \eta_2(r), \dots, \eta_p(r)) + \sum_{i=1}^p \frac{\kappa_i}{2} (\nabla \eta_i(r))^2 \right] d^3 r \quad (1)$$

where  $f(\dots)$  is the local free energy density,  $\eta_i$  are field variables,  $p$  is the number of field variables, and  $\kappa_i$  are the gradient energy coefficients. It is the gradient energy terms that give rise to grain boundary energies. For example, following the diffuse-interface theory of Cahn and Hilliard [25], the grain boundary energy,  $\sigma_{gb}$ , between a grain of orientation 1 and a grain of orientation 2 may be calculated as follows,

$$\sigma_{gb} = \int_{-\infty}^{+\infty} \left[ \Delta f(\eta_1, \eta_2) + \frac{\kappa_1}{2} \left( \frac{d\eta_1}{dx} \right)^2 + \frac{\kappa_2}{2} \left( \frac{d\eta_2}{dx} \right)^2 \right] dx \quad (2)$$

in which

$$\Delta f(\eta_1, \eta_2) = f(\eta_1, \eta_2) - f_{\min}$$

where  $f_{\min}$  represents the minimum of  $f(\eta_1, \eta_2)$ .

The relaxation kinetics of the field variables, and hence the grain boundary migration kinetics, are described by the continuum Cahn-Allen (Ginzburg-Landau) equations,

$$\frac{d\eta_i(r,t)}{dt} = -L_i \frac{\delta F}{\delta \eta_i(r,t)}, \quad i = 1, 2, \dots, p, \quad (3)$$

where  $L_i$  are the kinetic coefficients which describe the grain boundary mobilities. Substituting the free energy functional  $F$  in (1) into the kinetic equation (3) gives

$$\frac{d\eta_i}{dt} = -L_i \left[ \frac{\partial f(\eta_1, \eta_2, \dots, \eta_p)}{\partial \eta_i} - \kappa_i \nabla^2 \eta_i \right], \quad i = 1, 2, \dots, p \quad (4)$$

In this paper, I assume the following simple free energy density functional,

$$f(\eta_1, \eta_2, \dots, \eta_p) = \sum_{i=1}^p \left( -\frac{\alpha}{2} \eta_i^2 + \frac{\beta}{4} \eta_i^4 \right) + \gamma \sum_{i=1}^p \sum_{j \neq i} \eta_i^2 \eta_j^2 \quad (5)$$

where  $\alpha, \beta$ , and  $\gamma$  are phenomenological parameters. It should be emphasized that the absolute values of the phenomenological parameters and the gradient energy coefficients determine the grain boundary energies (equation (2)) as well as the boundary thickness. The most important requirement for the phenomenological parameters in (5) is that they provide a potential with  $2p$  potential wells. It may be easily shown that, if  $\gamma > \beta/2$ , the above free energy model has  $2p$  potential wells (minima) in the  $p$  field-variable space, which describe the equilibrium free energies of crystalline grains in  $2p$  different orientations. Under fixed values of the phenomenological parameters, both the grain boundary energies and boundary thickness can be adjusted by varying the gradient energy coefficients. The larger the gradient energy coefficients, the thicker the boundary thickness. In the limit of gradient energy coefficient going to zero, the boundary thickness becomes infinitely thin.

Using the free energy model (5), we arrive at the final set of kinetic equations,

$$\frac{d\eta_i}{dt} = -L_i \left[ -\alpha \eta_i + \beta \eta_i^3 + 2\gamma \eta_i \sum_{j \neq i}^p \eta_j^2 - \kappa_i \nabla^2 \eta_i \right], \quad i = 1, 2, \dots, p \quad (6)$$

For  $p = 1$ , the above set of equations describes the ordering and subsequent antiphase domain coarsening kinetics; for  $p = 2$ , it describes the ordering and interface migration kinetics which produces two different orientation variants; when  $p$  goes to infinity, the infinite set of equations describes the grain growth kinetics in a polycrystalline material.

To start a computer simulation, one may either input a pre-defined initial microstructure or generate the initial condition by assigning small random values to all the field variables at all positions, e.g., between - 0.01 and + 0.01. This initial condition simulates a liquid at a very high temperature.

For solving the set of kinetic equations (6), one needs to discretize it with respect to space. The Laplacian may be discretized by the following equation,

$$\nabla^2 \eta_i = \frac{1}{(\Delta x)^2} \left[ \frac{1}{2} \sum_j (\eta_j - \eta_i) + \frac{1}{4} \sum_{j'} (\eta_{j'} - \eta_i) \right] \quad (7)$$

where  $\Delta x$  is the grid size,  $j$  represents the set of first nearest neighbors of  $i$ , and  $j'$  is the set of second nearest neighbors of  $i$ . For discretization with respect to time, one may use the following simple Euler technique,

$$\eta_i(t + \Delta t) = \eta_i(t) + \frac{d\eta_i}{dt} \times \Delta t \quad (8)$$

where  $\Delta t$  is the time step for integration.

### Computer Simulation Results

All the results were obtained by using the discretization scheme (7) and (8) and by assuming,  $\alpha = 1.0$ ,  $\beta = 1.0$ ,  $\gamma = 1.0$ ,  $\kappa_i = 2.0$  for all  $i$  (isotropic grain boundary energy),  $\Delta x = 2.0$ ,  $\Delta t = 0.1$ ,  $L_i = 1.0$  for all  $i$  (isotropic grain boundary mobility). Periodic boundary conditions were applied along the two Cartesian coordinate axes.

#### Equilibrium Profiles of Field Variables Across a Straight Grain Boundary

To calculate the profiles of field variables across a straight grain boundary, a computation cell of  $200 \times 200$  lattice points was employed. A straight grain boundary was created in the middle of the cell by assigning to half of the lattice points  $\eta_1(r) = 1.0$  and  $\eta_{i \neq 1}(r) = 0.0$  and to the other half  $\eta_2(r) = 1.0$  and  $\eta_{i \neq 2}(r) = 0.0$ . Due to the periodic boundary condition, a second grain boundary was also created at the border of the computational cell. The profiles of  $\eta_1(r)$  and  $\eta_2(r)$  normal to the grain boundary obtained after 5000 time steps are shown in Fig. 1. The grain boundary width was found to be approximately 3 to 4 lattice planes (it is reminded that the lattice referred to in this paper is the lattice used to discretize the kinetic equations). The local free energy density,  $f(\eta_1, \eta_2)$ , across the grain boundary is shown in Fig. 2. With the information about the profiles of field variables and thus their gradients, and the local free energy density, the grain boundary energy can be calculated using equation (3). To visualize the microstructures, one may define the following function,

$$\psi(r) = \eta^2(r) = \sum_{i=1}^p \eta_i^2(r) \quad (9)$$

The values of  $\psi(r)$  normal to the grain boundary are shown in Fig. 3. For example,  $\psi(r)$  may be displayed by using gray-levels with low and high values represented by dark and bright colors, respectively. Since the values within the grains are close to 1.0, while those at the boundaries are significantly less, the bright regions will be grains and the dark lines will be grain boundaries. Using this representation, the microstructure with two straight grain boundaries is shown in Fig. 4.

#### Shrinking of a Circular Grain Embedded in an Infinite Matrix

As a first test of the kinetic equations (6) for studying grain growth, a circular grain of orientation 1 was embedded in an infinite matrix of orientation 2 as the initial condition. As expected, the circular domain shrank and finally disappeared in our computer simulation as shown in Fig. 5. The domain remained almost perfectly circular during the entire course of simulation until its disappearance. Furthermore, the grain boundary is very smooth. A plot of the circular domain area against time (Fig. 6) demonstrates that the area decreases linearly with time, indicating the dependence of

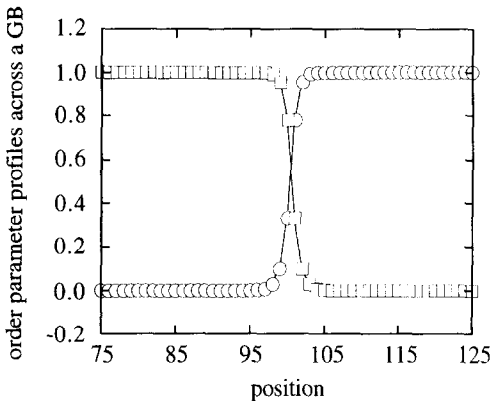


Fig. 1. Profiles of field variables across a grain boundary  
Open squares:  $\eta_1$ ; open circles:  $\eta_2$ .

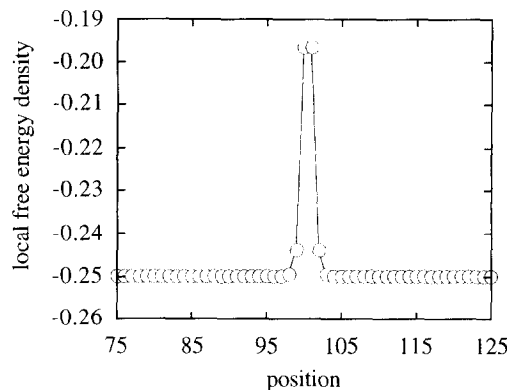


Fig. 2. The local free energy density across the grain boundary

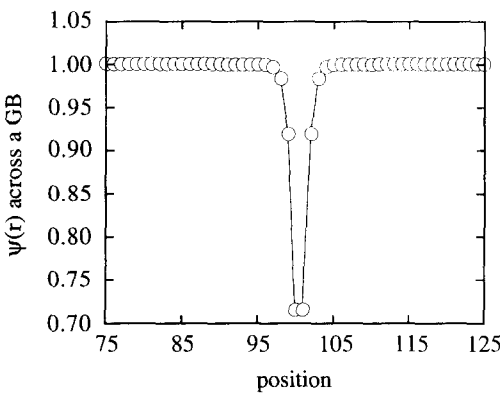


Fig. 3.  $\psi(r)$  across the grain boundary.

domain radius on time as  $t^{1/2}$ .

#### Grain Growth Kinetics Using 36 Field Variables

In this case, a computational cell of  $400 \times 400$  square lattice points was employed. The temporal microstructural evolution is shown in Fig. 7. The microstructures are remarkably similar to experimentally observed ones of normal grain growth in many single-phase polycrystalline materials. After about 1000 time steps, most boundaries become straight and meet at trijunctions. It is observed that shrinking and disappearance of small grains creates four-grain junctions which quickly split into two trijunctions due to their instability. Domain coalescence was occasionally observed although as many as 36 field variables were introduced.

The average grain size as a function of time was calculated by a computer counting of the size of each individual grain and the total number of grains at a given time. The average grain area in our two-dimensional system as a function of time is shown in Fig. 8. The data were obtained by averaging over 10 simulation runs starting with different initial

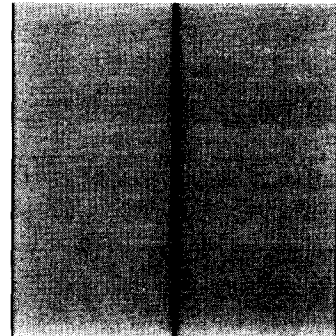


Fig. 4. Representation of a straight grain boundary

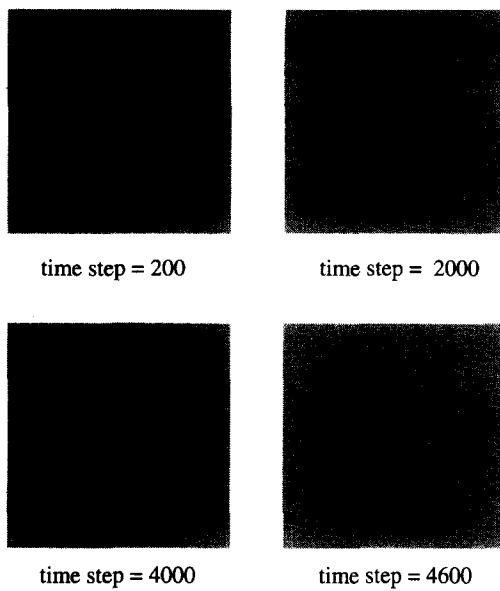


Fig. 5. Temporal evolution of a circular grain embedded in an infinite matrix.

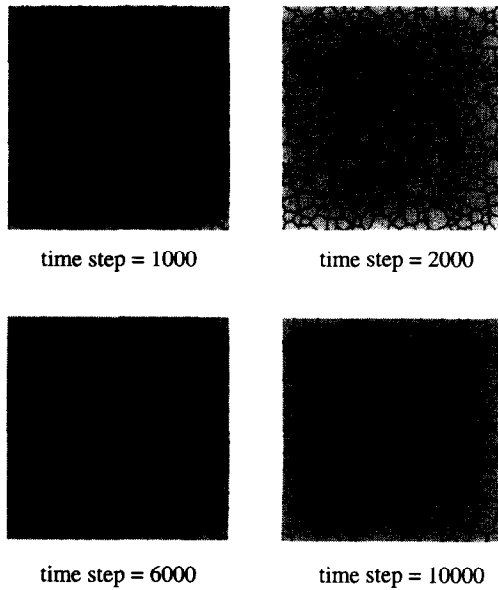


Fig. 7. Temporal evolution of microstructures using 36 field variables.

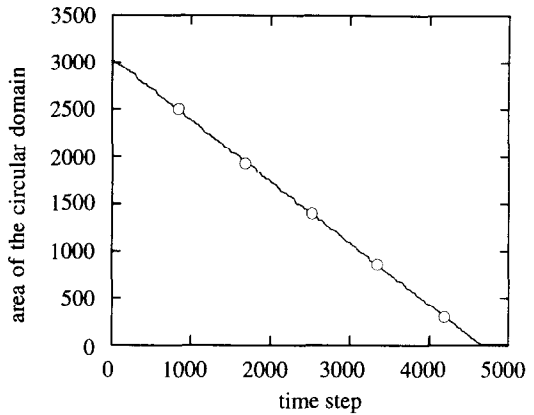


Fig. 6. The area of a circular grain embedded in an infinite matrix as a function of time.

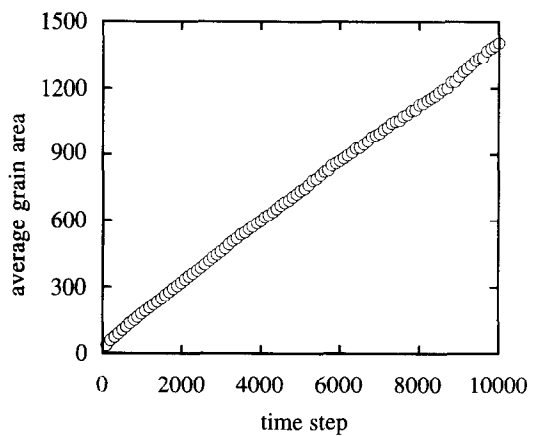


Fig. 8. Average grain area as a function of time for 36 field variables.

conditions. From careful analysis of the data [24], the time dependence of the average grain area was found to be linear, i.e., the average grain radius increases with time as  $t^{1/2}$ . The prediction of  $t^{1/2}$  dependence of average grain radius on time agrees with most of the previous mean-field and statistical theories of normal grain growth and more recent Monte-Carlo simulations based on the Q-state Potts model [22].

### Conclusions

A computer simulation model based on the continuum Ginzburg-Landau model with many non-conserved field variables is developed for investigating grain growth. The main features of this model include (1) grain boundaries are diffuse and smooth; and (2) with the input of initial microstructure and necessary parameters for specifying the grain boundary energy, it produces microstructural evolution automatically without tracking the positions of grain boundaries. All the statistical information about the microstructure such as the grain size distribution and topological distributions may be obtained. It is shown that the average grain radius increases with time as  $t^{1/2}$  during normal grain growth, which is the same as the time-dependence of the area-decrease of a single circular grain embedded in an infinite matrix.

### Acknowledgments

I am grateful to Dr. J. W. Cahn, A. G. Khachaturyan, W. C. Carter, G. L. Messing; and Mr. W. Yang, D. N. Fan, C. W. Geng and R. Poduri for very useful discussions. This work is supported by NSF under the grant number DMR 93-11898, by the Petroleum Research Fund administrated by the American Chemical Society, and by the ARPA/NIST program on mathematical modeling of microstructural evolution in advanced alloys. Computing time was provided by the Pittsburgh Supercomputing Center under Grant No. DMR 900022P.

### References

1. H. V. Atkinson, *Acta Metall.* **36**, 469 (1988).
2. J. E. Burke and D. Turnbull, *Prog. Metal Phys.* **3**, 220 (1952).
3. P. Feltham, *Acta Metall.* **5**, 97 (1957).
4. M. Hillert, *Acta Metall.* **13**, 227 (1965).
5. N. P. Louat, *Acta Metall.* **22**, 721 (1974).
6. C. S. Smith, *Metal Interfaces*, p. 65, ASM, Cleveland, OH (1952).
7. F. N. Rhines and K. R. Craig, *Metall. Trans.* **5A**, 413 (1974).
8. S. K. Kurtz and F. M. A. Carpay, *J. Appl. Phys.* **51**, 5745 (1980).
9. V. Yu. Novikov, *Acta metall.* **26**, 1739 (1978).
10. O. Hunderi, N. Ryum and H. Westengen, *Acta Metall.* **27**, 161 (1979).
11. O. Hunderi, and N. Ryum, *Acta Metall.* **29**, 1737 (1981).
12. D. Weaire and J. P. Kermode, *Phil. Mag.* **B48**, 245 (1983); *ibid*, **B50**, 379 (1984).
13. E. A. Ceppi and O. B. Nasello, *Scripta Metall.* **18**, 1221 (1984).
14. A. Soares, A. C. Ferro and M. A. Fortes, *Scripta Metall.* **19**, 1491 (1985).
15. V. E. Fradkov, L. S. Shvindlerman and G. G. Udler, *Scripta Metall.* **19**, 1285 (1985).
16. V. E. Fradkov, A. S. Kravchenko and L. S. Shvindlerman, *Scripta Metall.* **19**, 1291 (1985).
17. H. J. Frost, C. V. Thompson, and D. T. Walton, *Acta Metall. et Maters* **38**, 1455 (1990).
18. J. Wejchert, D. Weaire and J. P. Kermode, *Phil. Mag.* **B53**, 15 (1986).
19. P. S. Sahni, G. S. Grest and S. A. Safran, *Phys. Rev. Lett.* **50**, 263 (1983).
20. D. J. Srolovitz, M. P. Anderson, G. S. Grest and P. S. Sahni, *Scripta Metall.* **17**, 241 (1983).
21. M. P. Anderson, D. J. Srolovitz, G. S. Grest, and P. S. Sahni, *Acta Metall.* **32**, 783 (1984).
22. G. S. Grest, M. P. Anderson and D. J. Srolovitz, *Phys. Rev. B* **38**, 4752 (1988).
23. S. Ling and M. P. Anderson, *JOM*, **9**, 30 (1992), and references therein.
24. L. Q. Chen and W. Yang, to be published in *Phys. Rev. B*, (1994).
25. J. W. Cahn and J. E. Hilliard, *J. Chem. Phys.* **28**, 258 (1958).